frontiers | Frontiers in Earth Science

TYPE Original Research
PUBLISHED 11 March 2024
DOI 10.3389/feart.2024.1377738

OPEN ACCESS

EDITED BY
Xixin Wang,
Yangtze University, China

REVIEWED BY
Luxing Dou,
Yangtze University, China
Long Luo,
Chongqing University of Science and Technology, China

*CORRESPONDENCE
Zhuang Liang,
13206822011@163.com

RECEIVED 28 January 2024
ACCEPTED 23 February 2024
PUBLISHED 11 March 2024

CITATION
Li G, Li C, Zhang B, Zhang L, Liang Z and Chen Q (2024), Characterization of reservoir quality in tight sandstones from the Benxi Formation, eastern Ordos Basin, China. *Front. Earth Sci.* 12:1377738. doi: 10.3389/feart.2024.1377738

Characterization of reservoir quality in tight sandstones from the Benxi Formation, eastern Ordos Basin, China

Guoyong Li[1], Cong Li[1], Boming Zhang[1], Lei Zhang[2], Zhuang Liang[3,4]* and Qi Chen[3,4]

[1]China National Petroleum Corp, JiDong Oilfield, Tangshan, Hebei, China, [2]Luliang Oilfield Operation Area of Xinjiang Oilfield Branch Company, PetroChina, Karamay, China, [3]State Key Laboratory of Petroleum Resources and Prospecting, China University of Petroleum (Beijing), Beijing, China, [4]College of Geoscience, China University of Petroleum (Beijing), Beijing, China

The Benxi Formation in the eastern Ordos Basin harbors abundant natural gas resources and shows promising exploration and development potential. However, the reservoir characteristics are complex, and the primary controlling factors are unclear, presenting significant challenges for reservoir characterization. In response to these challenges, we conducted a systematic study on the characteristics of tight sandstone reservoirs in the Benxi Formation by integrating thin section analysis, scanning electron microscopy, high-pressure mercury injection, and conventional petrophysical analysis alongside well log data analysis. By applying empirical calculation formulas of a porosity evolution quantitative model, we elucidated the primary controlling factors of reservoir heterogeneity. Our research identified that the reservoirs in the eastern Ordos Basin, Benxi Formation, are predominantly composed of quartz sandstone and lithic quartz sandstone, with pore-filling cementation as the dominant cement type and the main storage spaces being intergranular pores and dissolved pores. The homogenization temperatures of fluid inclusions in authigenic quartz range from 92.8 to 185.7°C, indicating that the target layer is in the mesodiagenesis phase B. The main reasons for the differences in reservoir quality in the Benxi Formation are attributed to both sedimentation and diagenesis. In terms of sedimentation, two distinct sedimentary microfacies control the distribution of reservoir quality differences based on variations in quartz content and soluble components. Regarding diagenesis, the Benxi Formation underwent compaction, cementation, and dissolution, with compaction being the fundamental cause of widespread reservoir compaction.

KEYWORDS

Ordos Basin, Benxi Formation, reservoir quality, tight sandstone reservoirs, diagenesis

1 Introduction

The Benxi Formation in the Ordos Basin is a deep-buried reservoir of the Paleozoic era, with high natural gas reserves and an unobstructed flow rate exceeding 50 × 104 m^3/day (Jia et al., 2019a; Jia et al., 2019b; Li et al., 2021; Wang et al., 2021a). Therefore, the Benxi Formation is an important potential alternative area for increasing oil and gas reserves and

production. However, due to the complex composition, high quartz content, and strong diagenesis of the Benxi Formation, the reservoir exhibits strong heterogeneity and complex pore structures, thus limiting the exploration and development of natural gas (Li et al., 2021; Wang et al., 2021b).The rigid compressive strength of quartz inhibits compaction and leads to a significant amount of residual intergranular pores. These pore spaces are conducive to the entry of acidic fluids and the development of dissolution processes. Acidic fluids dissolve quartz and other detrital particles (Colo n et al., 2004; Crundwell, F, 2014; Wang et al., 2020a), connecting isolated pores and increasing the secondary porosity of the rock. This is a key factor affecting the overall porosity and permeability of tight sandstones (Li et al., 2020; Panagiotopoulou et al., 2007; Pokrovsky et al., 2009).

During a specific period, the Benxi Formation exhibits significant variations in unstable mineral composition and diagenetic fluid properties. Unstable components in feldspar and rock fragments are commonly dissolved in an acidic environment, leading to the formation of dissolution pores and casting pores within the grains, typically during the early to middle diagenetic stages. In contrast, quartz and other silicate minerals dissolve mainly during the late to post-diagenetic stages (Crundwell, 2014; Panagiotopoulou et al., 2007). Compaction, dissolution, and cementation processes interact with each other. The residual intergranular pores formed as a result of mechanical compaction provide favorable pathways for acidic fluids, while the unstable components in early sediments serve as the material basis for dissolution processes, thereby improving reservoir quality. Conversely, clay minerals (such as illite, kaolinite, and quartz cement) resulting from dissolution remain in the pores of tight sandstone reservoirs, hindering the flow of diagenetic fluids (Zhong et al., 2007; Gao et al., 2020; Hong et al., 2020; Wang et al., 2022; Morad et al., 2010; Taylor et al., 2010). Due to the fact that the tight sandstone reservoirs within the Benxi Formation are situated in a high-acidity environment formed within coal-bearing strata from source rocks (Li et al., 2021; Wang et al., 2021c), it is crucial to clarify the diagenetic evolution sequence, the contributions of various diagenetic processes to reservoir quality, and the controlling factors in order to promote efficient exploration in the Benxi Formation oil and gas development area.

This study combines experimental and theoretical approaches to investigate the quality characteristics of the Benxi Formation reservoir and the controlling factors of quality variations in tight sandstone reservoirs in the eastern Ordos Basin. Thin section analysis, core petrophysical analysis, and scanning electron microscopy (SEM) were used to conduct in-depth investigations into the reservoir types, structural features, composition of detrital particles, and cementation of the rocks. Based on the Scherer initial porosity recovery model (Scherer, 1987) and the Paxton and Ehrenberg compaction porosity loss formula, the primary controlling factors of diagenetic processes were determined by calculating the decrease in porosity based on compaction and cementation processes (Scherer, 1987; Ehrenberg, 1990; Ehrenberg et al., 2009; Paxton et al., 2002). The aim was to clarify the characteristics of sandstone reservoirs, describe the process of reservoir densification, and elucidate the evolution of primary and secondary porosity based on consideration of both sedimentation and diagenesis. Moreover, the study analyzed the influence of geological factors (such as grain size, mineral content, and diagenetic processes) on the reservoir quality of the Benxi Formation. The findings of this research can provide a basis for the prediction of favorable reservoirs in the eastern Ordos Basin.

2 Geological background

The Ordos Basin is located in the western part of the North China Block (Figure 1A). It is a poly-cycle cratonic basin with a north-south uplift, a long and gentle eastern flank, and a short and steep western flank. It can be divided into six tectonic units: the Yimeng Uplift, the Jinxi Tectonic Zone, the Weibei Uplift, the Western Thrust Zone, the Tianhuan Depression, and the Yishan Slope (Lin et al., 2013; Wang et al., 2017) (Figure 1B).

The research area is located in the northeastern part of the Yishan Slope in the Ordos Basin, located between 37° 41′47″ ~ 38° 23′34″N, 110° 0′45" ~ 110° 45′10″E. Administratively, it is within the boundaries of Shenmu County, Jia County, and Mizhi County in Yulin City, Shanxi Province. The stratigraphic formation in this area is the tight sandstone reservoir of the Benxi Formation in the Carboniferous (Figures 1C, D; Wang et al., 2017).

The top coal seams of the Benxi Formation are in conformable contact with the sandstone or mudstone of the Taiyuan Formation and are unconformably in contact with the lower Ordovician Majiagou Formation limestone (Wang et al., 2017). The thickness of the formation ranges from 27.8 to 82.8 m, with an average of 51.9 m (Figure 2). During the sedimentation period of the Benxi Formation, the tectonic stability was high, and the topography was relatively flat. The predominant sedimentary environment was tidal flat depositional with minor influences of shoreline, tidal channel, sand flat, mud flat, and swamp microfacies types (Jia et al., 2019a; Jia et al., 2019b; Lin et al., 2013). Among them, the tidal channel and sand flat are favorable for the development of tight sandstone reservoirs within the Benxi Formation. The mud flat and swamp, including the coal seams, serve as good hydrocarbon source rocks and are the primary contributors to the tight sandstone gas in the Benxi Formation.

3 Data and experiments

3.1 Data

A total of 22 cylindrical sandstone samples were collected from the target formation in 65 wells in the Jiaxian Block. Each sample had a diameter of 2.5 cm and a length of 8 cm, obtained by vertically drilling fresh core plugs from the wellbore. Additionally, pore volume and permeability data were collected for 134 samples from the Jidong branch of PetroChina, CTS analysis for 205 samples, SEM data for 20 samples, and cathodoluminescence (CL) data for 17 samples.

Prior to experiments, the 22 samples underwent washing to remove residual hydrocarbons and were subsequently dried at 120°C for 48 h. Initially, the samples were tested for pore volume and permeability. Then, a 0.5 cm length was cut from the top of each sample for CTS observation to investigate the lithological characteristics, pore morphology, and genetic types of different samples. Based on the physical properties and CTS assessment,

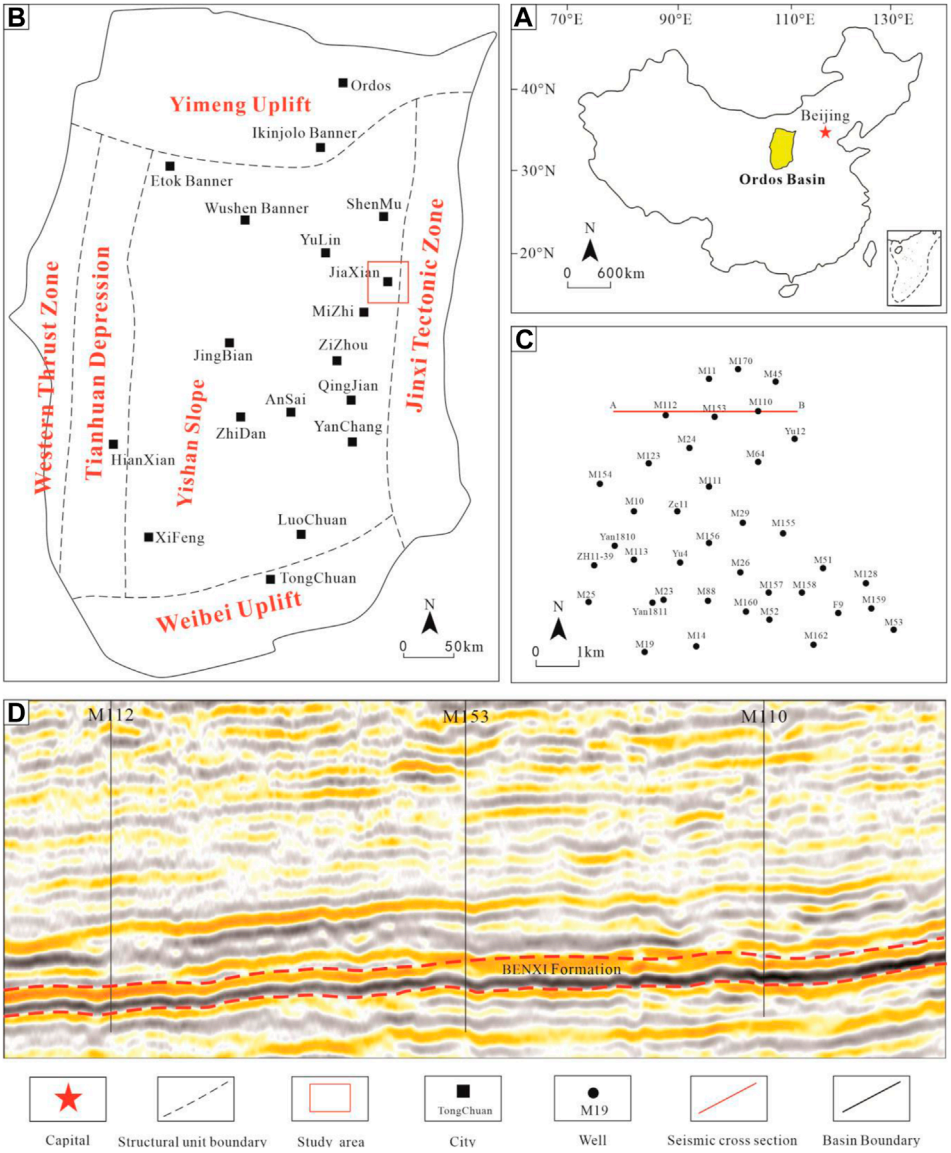

FIGURE 1
(A) Geographical location map of Ordos Basin **(B)** Structural location map of Ordos Basin (Lin, J et al., 2013) **(C)** Well location in the study area **(D)** Seismic cross section of AB connection in Figure 1C.

eight representative samples were selected and sliced into 2.5 cm and 5 cm sections. The SEM observation was conducted on the 2.5 cm sections of the eight samples. Subsequently, fluid inclusion tests were conducted on the 5 cm sections of the same eight samples. Detailed information for each experiment is described as follows.

3.2 Experiments

3.2.1 Well-logging data analysis

The log curves of the development wells in the study area were systematically analyzed using Petrel 2018 software and Resforrm V3.5 software. Firstly, the GR, RT and AC log curves were normalized to ensure consistency among the different units. Next, these three log curves were utilized to distinguish lithological formations such as sandstone, mudstone, coal, and limestone. Sandstone exhibits low GR, low RT, and low AC values, while coal displays low GR, high RT, and high AC values. Limestone is characterized by low GR, low RT, and high AC values, while other formations are identified as mudstone. After distinguishing the lithological formations, the rhythmic patterns of the GR curve and sandstone thickness were used to determine the sedimentary facies type, providing fundamental data for subsequent reservoir quality studies.

3.2.2 Core physical property test

A CMS~300 apparatus was used to test porosity and permeability at the State Key Laboratory of China University of Petroleum-Beijing (CUPB). The helium dilation method and the

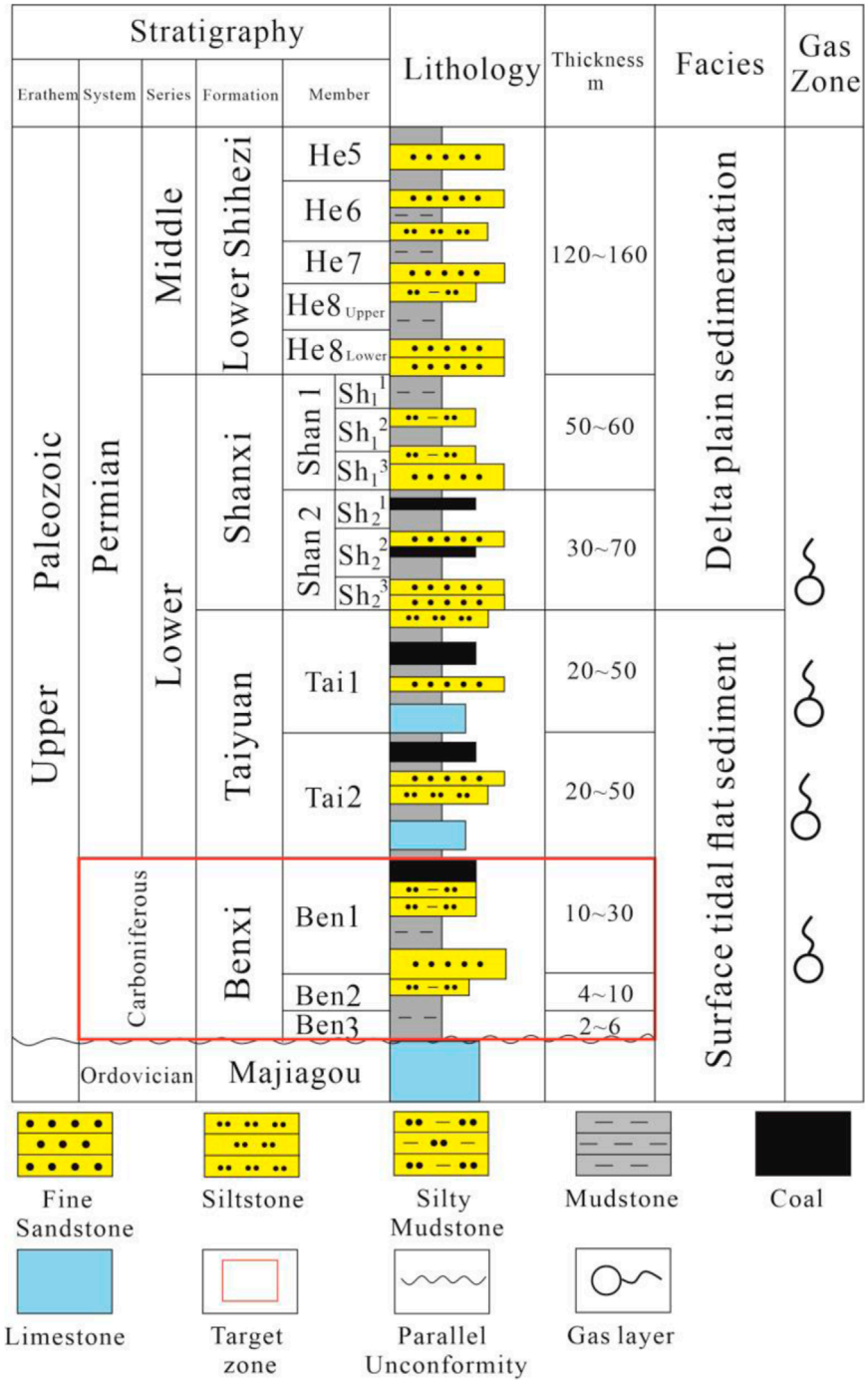

FIGURE 2
Stratigraphic overview map of the study area (Wang, F et al., 2017).

dynamic pressure method were used to measure porosity and permeability, respectively, Klinkenberg calibration was performed during the permeability measurement, which was performed at the ambient temperature of 23°C, the humidity of 61% and the conffning pressure of 97.2 kPa by SY/T 5336–1996. Through core porosity and penetration rate testing, understand the core physical property and reservoir properties in the study area.

3.2.3 CTS and SEM

Polished thin sections with a thickness of 0.3 mm were impregnated with blue resin and analyzed using a polarizing microscope (ikLV100nPOL) to examine the rock composition, pore and throat types, morphology, particle sorting, abrasion, and fracturing. The point counting method was employed to study the rock composition, pore and throat types, morphology, particle

classification, abrasion, and cementation of the sandstone samples. Generally, a minimum of 200 points were quantified for each sample. The statistical error for each microphotograph was less than 2%. Testing was done according to the SY/T 5368~2016 standard. Scanning electron microscope (SEM) analysis was performed using a Quanta~200 FESEM with a maximum resolution of 1.2 nm. SEM analysis provided high-resolution micrographs, including high-resolution microimages of pores and throats, intercrystalline micropores of authigenic and clay minerals, and further insights into mineral paragenetic sequences, clay mineral morphological sequences, clay mineral morphologies, pore sizes, and connectivity.

3.2.4 Fluid inclusions

Polished thin sections with a diameter smaller than 20 mm were placed on the stage of the microscope for microscopic observation of fluid inclusions in quartz. The main observations focused on the occurrence state, inclusion types, size and shape, distribution characteristics, and gas phase percentage within the inclusions. This allowed for the selection of suitable fluid inclusion samples for subsequent testing and analysis.

Microthermal analysis was conducted on the selected fluid inclusion samples using a Linkam TH600 stage. By measuring the low-temperature phase transition temperature and homogenization temperature of the inclusions, information on fluid salinity and the minimum trapping temperature of the inclusions was obtained. The testing was conducted in accordance with the SY/T 6010~2011 standard.

Homogenization temperature analysis of fluid inclusions provides insights into determining the main mineralization period or mineralization stage and their chronological sequence. Additionally, it aids in further studying the diagenetic stages and diagenetic processes.

3.2.5 HPMI

The HPMI experiment was conducted with an AutoPore IV9505 mercury porosimeter at the Analysis and Test Center of Exploration and Development Research Institute of China Changqing Oilfield Company.

The test standard is according to Chinese standard SY/T 5346–2005. The eight cylindrical samples had a diameter of 2.5 cm and a length of 3.0 cm. The highest mercury intrusion pressure was set to 200 MPa, and the corresponding pore radius was 0.0037 μm, which was the smallest pore radius obtained in the test. After the mercury injection pressure reaches the maximum, the pressure progressively declines and the mercury is withdrawn from the sample. The HPMI test can acquire the capillary pressure vs mercury saturation curve during mercury intrusion and extrusion. The equivalent pore throat radius of capillary pressure can be computed using the Washburn equation. Finally, multiple characteristic parameters representing pore size distribution can be obtained.

4 Results

4.1 Reservoir lithological

Based on the identification of cast thin sections and whole-rock X-ray diffraction, the Benxi Formation tight sandstone reservoir consists of three types: quartz sandstone, lithic quartz sandstone, and lithic sandstone (Li et al., 2021; Wang et al., 2021c; Hu et al., 2019). Lithic quartz sandstone and lithic sandstone are the predominant types, accounting for 50.9% and 33.5% of the total samples, respectively. Quartz sandstone is less abundant, accounting for only 15.6% (Figure 3). The composition of sandstone clasts is primarily quartz, with an average content of 70.9%. The content of lithic clasts is relatively low, at 29.05%. Feldspar content is minimal or absent (Table 1). There are various types of lithic clasts, mainly including schist clasts and quartzite clasts, followed by phyllite, slate, and metamorphic sandstone, with occasional occurrences of pyrite, siderite, and other minerals. The overall sandstone is mainly composed of medium to fine sandstone, showing moderate to good sorting, particle support, linear-convex contacts, and predominantly pore-filling cementation. The sandstone exhibits a high level of compositional maturity and structural maturity.

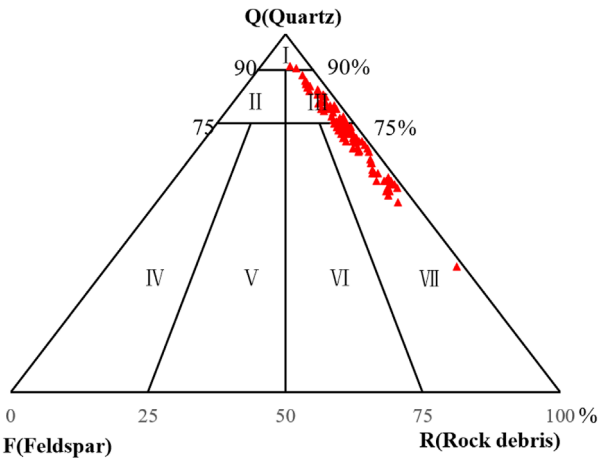

FIGURE 3
Triangular diagram of sandstone composition of Benxi Formation. Number of samples = 110. I-Quartz sandstone; II-Feldspar quartz sandstone; III-Lithic quartz sandstone; IV-Feldspar sandstone; V-Lithic feldspar sandstone; VI-Feldspar lithic sandstone; VII-Lithic sandstone.

The main cementing material in the tight sandstone is clay minerals, with kaolinite having the highest average content at 46.1%, followed by illite at 31.2%. The interlayered illite/smectite and chlorite have contents of 17.8% and 4.9%, respectively (Figure 4). As the Benxi Formation was deposited in a marine environment, abundant Ca^{2+} and Mg^{2+} ions provided by seawater promoted the development of various types of carbonate cements, such as calcite and dolomite (Hu et al., 2019; Wang et al., 2021). Through the observation of cast thin sections and scanning electron microscope analysis, worm-like kaolinite (Figure 5A) and needle-like chlorite, as clay minerals, were identified as authigenic fills in the pores. Iron-bearing calcite (Figure 5B) and iron-bearing dolomite (Figure 5C) are the main carbonate cements, with iron-bearing calcite replacing clasts and iron-bearing dolomite filling the pores in a pseudomorphic manner (Figures 5D, E). Sporadic occurrences of pyrite are found between intergranular pores (Figure 5F).

10.3389/feart.2024.1377738

TABLE 1 Composition table of sandstone clastic particles in Benxi Formation.

Well	Sample numbers	Quartz (%)	Feldspar (%)	Rock debris (%)	Quartzite (%)	Phyllite (%)	Metasandstone (%)	Slate (%)
M46	202,308,006	53	0	47	12	2	0	0
F9	202,308,007	64	0	36	4.5	1.5	2	0.5
M51	202,308,008	72	0	28	6	2	1	1
M51	202,308,009	74	0	26	7	0	0	0.5
M158	202,308,010	81	0	19	3	0	0.5	0
M161	202,308,011	71	0	29	17	0	0.5	0

4.2 Reservoir pore structure

The pore types in the Benxi Formation sandstone include primary pores (intergranular pores), secondary pores (intergranular dissolution pores, feldspar dissolution pores, lithic clasts dissolution pores, miscellaneous substance dissolution pores), intercrystalline pores, and microfractures, totaling five types (Figure 6). Intergranular pores generally range from 0.2% to 3.5%, with an average of 1.2%. Secondary pores are distributed between 0.1% and 4.8%, with an average of 1.27%, mainly consisting of intergranular dissolution pores and lithic clasts dissolution pores (Hu et al., 2019). Intercrystalline pores and microfractures are less abundant, accounting for an average of 0.3%. Intergranular pores and dissolution pores serve as the primary reservoir spaces in the tight sandstone reservoir of the Benxi Formation.

4.3 Porosity and permeability

Based on the core analysis test data from 404 core samples taken from 14 wells, the porosity of the Benxi Formation sandstone ranges from 0.23% to 13.77%, with an average of 6.2%. The permeability ranges from 0.002 to 12.56 × 10^3 μm^2, with an average of 1.35 × 10^3 μm^2, indicating that it belongs to low porosity and extremely low permeability reservoirs (Figure 7A). Additionally, there is a significant positive correlation between porosity and permeability (Figure 7B), indicating that the reservoir in the Benxi Formation has a simple pore-throat structure, and its reservoir properties are mainly determined by the size of the pore space.

Based on the analysis of high-pressure mercury intrusion pore-throat parameters, the Benxi Formation tight sandstone reservoir exhibits relatively large median pore-throat radius, close to unity sorting coefficient, indicating moderate to good pore-throat sorting and a concentrated distribution (Table 2). Overall, the reservoir shows good homogeneity. The skewness of the throats is not significant, suggesting that the throat sizes are biased towards larger throats compared to the average throat radius. The displacement pressure is relatively low, indicating the presence of larger maximum connected pore-throat radius and good reservoir permeability. The maximum mercury saturation is relatively high, reflecting the reservoir's good storage capacity.

4.4 Fluid inclusions

Based on fluid inclusion test data, it is observed that fluid inclusions are mainly distributed within dissolution pores or fractures within quartz grains, often appearing as irregular gas-liquid two-phase inclusions. Inclusions in the cementing material are rarely encountered. The quantity of fluid inclusions is moderate, with well-developed quartz triple junctions. There are two main stages: early-stage inclusions are found within early-stage fractures of quartz grains, which are narrow and contain relatively smaller individual inclusions. Late-stage inclusions are distributed within dissolution pores or late-stage fractures within quartz grains, showing a good fluorescent response.

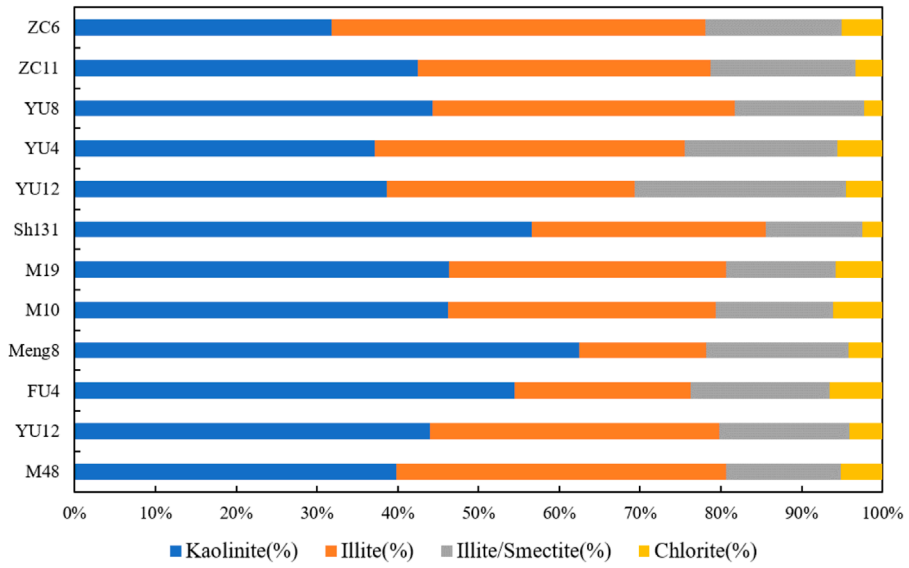

FIGURE 4
Microscopic characteristics of Benxi Formation reservoirs in JiaXian area.

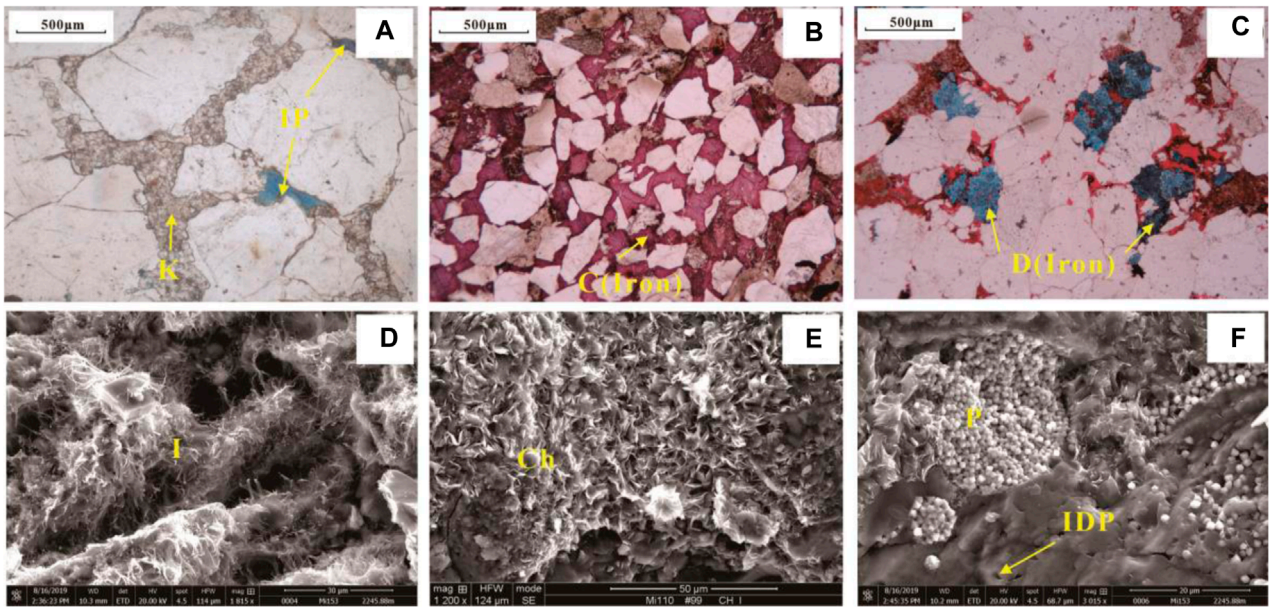

FIGURE 5
Microscopic characteristics of Benxi Formation reservoirs in JiaXian area **(A)** Sub-angular-sub-circular quartz grains, intergranular filling with worm-like kaolinite, Well M51, 2158 m, (–); **(B)** Iron-bearing calcite cementation, Well M112, 2091 m, (–); **(C)** Iron-bearing dolomite, Well M128, 2006 m, (–); **(D)** Filamentous illite, Well M157, 2060 m, (–); **(E)** Scaly chlorite, Well M110, 2105 m, SEM; **(F)** Pyrite filling and intergranular dissolution, Well M158, 2110 m, SEM. IP=Intergranular pore, C (Iron)=Iron-bearing calcite, D (Iron)= Iron-bearing dolomite, I= illite, Ch= chlorite, P= Pyrite, IDP= Intergranular dissolution pore, K= Kaolinite.

Experimental results demonstrate that the fluid inclusions in the reservoir sandstone exhibit a uniform temperature distribution, ranging from 92.8°C to 185.7°C (Figure 8). The reservoir in this area has undergone two distinct peaks at around 120 ~ 130°C and 150 ~ 160°C, indicating two hydrocarbon charging events in the evolution from early diagenesis to mesodiagenesis (Wang et al., 2021).

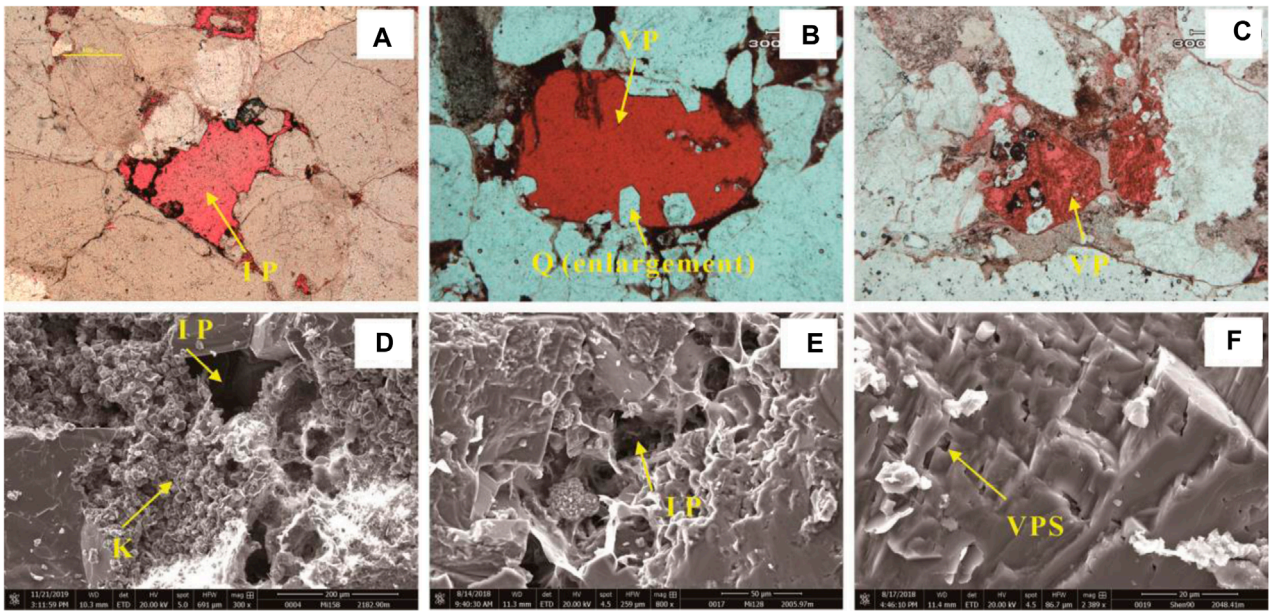

FIGURE 6
Microscopic Characteristics of Pore Structure of Benxi Formation Sandstone **(A)** Residual Intergranular Pores, Well M52, 2018 m, (–); **(B)** Rock debris dissolution pores, Well M7, 2168 m, (–); **(C)** Rock debris dissolution pores, Well M26, 2136 m, (–); **(D)** Residual Intergranular Pores, Well M158, 2182 m, SEM; **(E)** Kaolinite dissolution, Residual Intergranular Pores, Well M23, 2115 m, SEM; **(F)** Iron-bearing calcite dissolution pores, Well S90, 2048 m, SEM. IP= Intergranular Pores, VPS=Vugular pore space, Q (enlargement)= Quartz enlargement, K= Kaolinite.

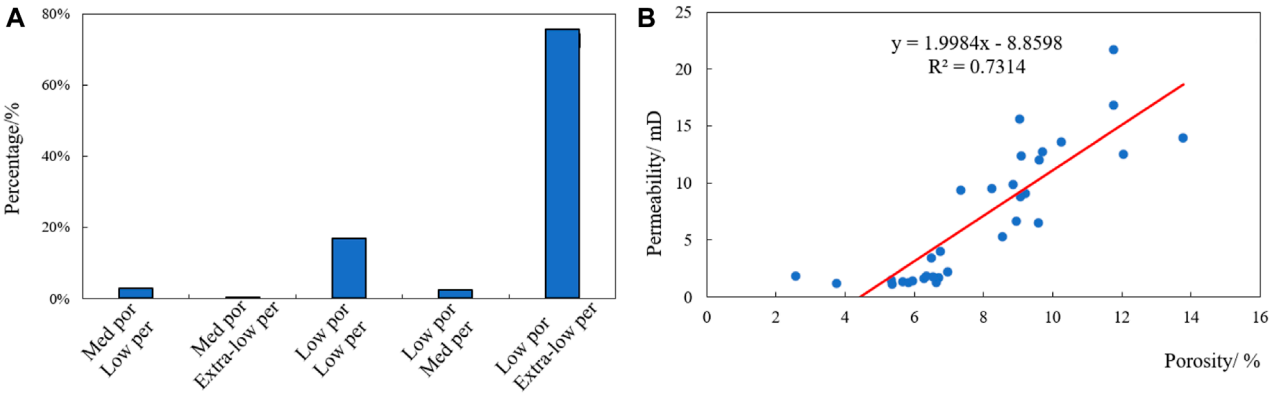

FIGURE 7
Statistical chart of reservoir characteristics and pore types. **(A)** Histogram of reservoir type; **(B)** Histogram of porosity and permeability.

5 Discussion

5.1 Sedimentation controls the material composition of the reservoir

Sedimentation processes do not directly impact reservoir quality. They influence reservoir quality through the macroscopic control of rock grain size and composition, which further affects the diagenetic processes of sediment and ultimately influences reservoir quality. In general, diagenetic processes are the direct factors that impact reservoir quality.

5.1.1 Rock grain size controls reservoir physical properties

Sedimentary processes have an inherent control on reservoirs. Sediments possess numerous primary pores, and their size and distribution are controlled by sedimentary facies. Coarser-grained rocks with lower mud content generally exhibit better original porosity and permeability (Wang et al., 2021c). Experimental studies on reservoir properties of different rock facies provide values for porosity and permeability. Among these facies, coarse sandstone exhibits the highest porosity and permeability, with average values of 9% and 1.01 mD, respectively. Fine sandstone, on the other

TABLE 2 High pressure mercury injection curve parameter table.

Well	Depth (m)	Displaceme pressure (MPa)	Median radius (μm)	Maximum mercury saturation (%)	Mercury removal efficiency (%)	Mean value	Skewness	Sorting coefficient
S90	2048.41	1.42	0.18	86.72	37.33	11.89	1.25	1.25
S90	2051.20	0.31	0.89	94.31	36.54	9.89	1.74	1.15
M128	2003.04	0.35	0.90	89.62	20.96	10.04	1.88	1.38
M128	2014.01	0.42	0.76	87.73	24.58	10.25	1.81	1.32
M51	2149.48	0.27	0.13	93.30	30.59	11.95	2.68	1.28
M51	2157.86	0.40	0.17	90.56	31.29	11.41	2.48	1.49
M46	2252.30	0.05	1.09	87.97	40.10	9.52	2.49	1.49
M26	2311.10	8.13	0.09	78.78	38.89	9.71	1.51	1.27

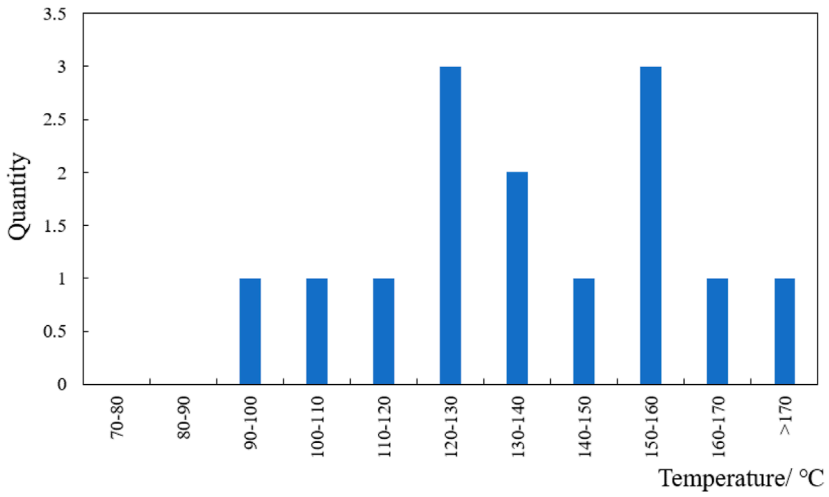

FIGURE 8
Fluid inclusion homogeneous temperature histogram.

hand, has the lowest original porosity, with an average of 2.3% (Figures 9A, B).

Furthermore, grain size also influences diagenetic processes. Coarse sandstone is formed in high-energy water environments with strong transportation capacity and good continuity, making it difficult for some weakly compactable detrital or plastic minerals to be preserved. Thus, the original sediment of coarse sandstone exhibits strong compaction resistance (Figure 9C). As a result, the remaining original porosity is relatively high, facilitating dissolution and cementation processes. Conversely, fine-grained sandstones have weak compaction resistance, resulting in very limited residual pore space after compaction, which hinders fluid flow during diagenesis, leading to relatively weaker cementation and dissolution processes (Figure 9D).

5.1.2 Sedimentary facies determine the material composition of rocks

The overall development of lagoonal tidal flat sedimentation is observed in the study area, but the reservoir performance of various microfacies within it shows some variations. Quartz sandstone exhibits relatively good reservoir performance, followed by lithic quartz sandstone, and lithic sandstone has the poorest performance (Table 3). The development and distribution of these rock types are clearly controlled by sedimentary microfacies (Wang et al., 2021a; Hu et al., 2019; Dutton and Loucks, 2010).

Two main types of microfacies are developed in the reservoir interval within the study area, and they exhibit distinct reservoir characteristics (Figure 10). The first type is the tidal channel microfacies of the subtidal zone, characterized by thicker channel sand bodies that are laterally limited and only developed in the

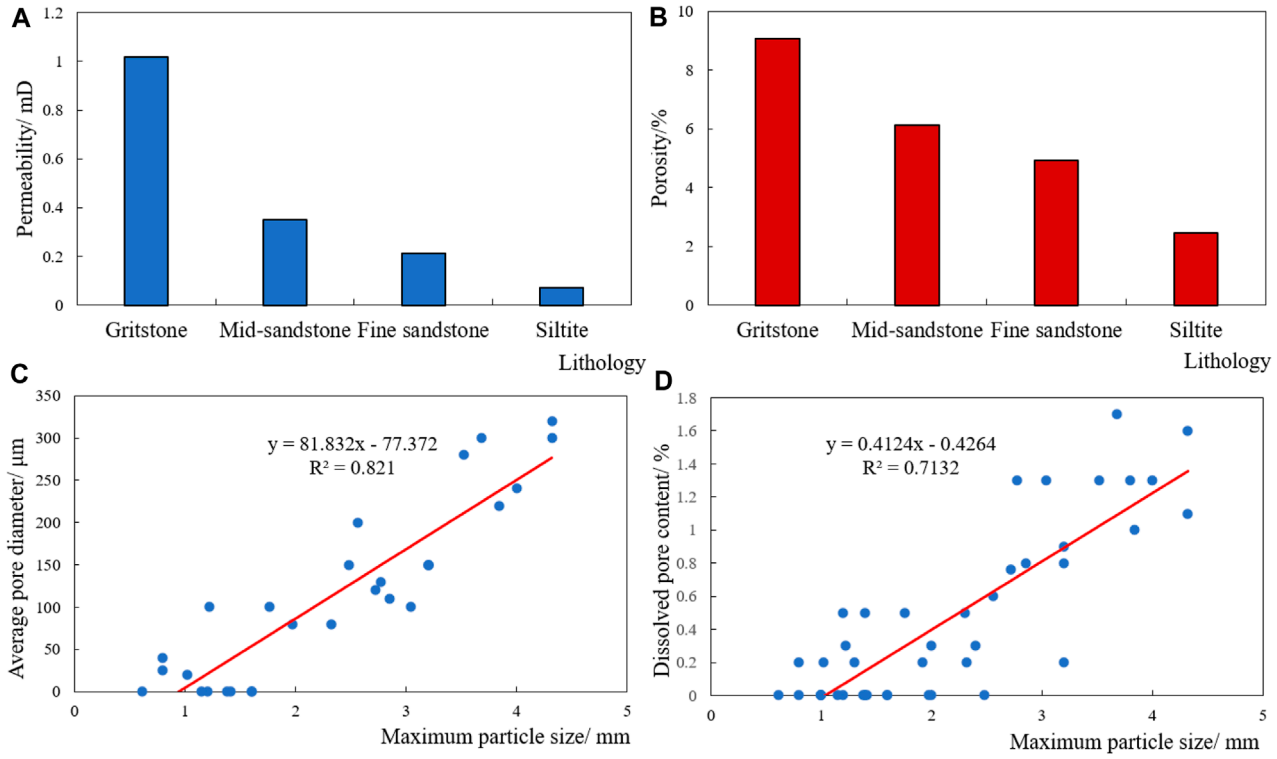

FIGURE 9
Physical properties of reservoirs of different lithologies in the Benxi Formation. **(A)** Histogram of lithology and permeability; **(B)** Histogram of lithology and porosity; **(C)** Relationship between maximum particle size and average pore size; **(D)** Relationship between maximum particle size and dissolved pore content.

TABLE 3 Rock type reservoir quality difference table.

Sedimentary facies type	Sandstone type	Porosity (%)	Permeability (10^{-3} μm^2)	Media radius (μm)	Sorting coefficient	Variable coefficient	Displacemen pressure (MPa)	Maximum mercury saturation (%)
Tidal channel microfacies	Quartz sandstone	9.6	1.95	0.67	2.21	0.22	0.27	86.85
Sand flat microfacies	Lithic Quartz Sandstone	7.1	1.27	0.45	2.38	0.21	0.35	78.35
Sand flat microfacies	Lithic Sandstone	5.02	0.59	0.2	1.85	0.15	0.79	83.1

southern part of the study area. The bottom of the channel shows evidence of finer gravel lag deposits, transitioning upward to medium to coarse sandstone, with a sharp top, exhibiting a well-defined box-shaped log response. The tidal channel microfacies experience turbulent water flow and strong hydraulic energy, as the clastic particles have undergone prolonged scouring, resulting in a relatively low content of unstable rock fragments. The dominant lithology is quartz sandstone, with abundant intergranular volume, facilitating the entry of acidic fluids and exhibiting good porosity and permeability. It is considered the highest-quality reservoir in the area.

The second type is the sand flat microfacies of the intertidal zone, characterized by thinner sand bodies and interbedded sand and mud. They are laterally extensive and widespread throughout the study area. Similar to the tidal channel microfacies, the bottom of the sand flat microfacies shows evidence of lag deposits, transitioning upward to medium to fine sandstone, with a gradual top and log response exhibiting a box-shaped or bell-shaped curve with significant notching. The sand flat microfacies are located in the intertidal zone, where the water is relatively stable compared to the subtidal zone, allowing for ample deposition of clastic material. The dominant lithologies are lithic quartz sandstone and quartz

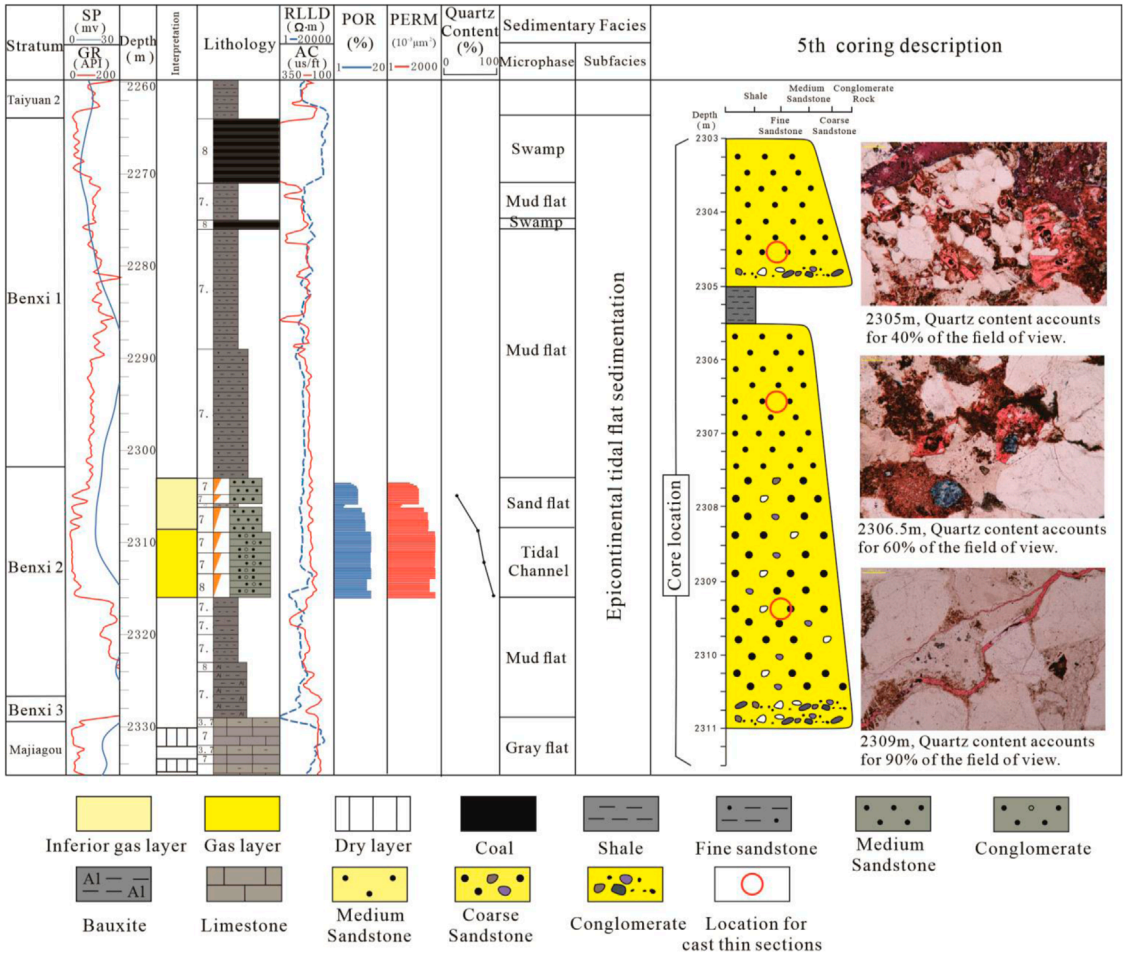

FIGURE 10
Columnar diagram of core from Benxi Formation, Well M26.

sandstone, with moderate porosity and permeability, making them the most well-developed reservoirs in the area.

5.2 Diagenesis controls the differential characteristics of reservoirs

5.2.1 Diagenetic stage of reservoir

In the study area, the burial depth of the Benxi Formation ranges from 2300 to 3400 m (Wang et al., 2021b; Hu et al., 2019). The vitrinite reflectance (Ro) of the samples is between 1.3% and 2.0% (Li et al., 2021) The ratio of I/S is less than 10%. The fluid inclusions in authigenic quartz exhibit a uniform temperature range of 100°C–170°C. According to the SYT5477-2003 petroleum industry standard, the target interval is in the mesodiagenesis B (Figure 11). A comprehensive study has been conducted on the diagenetic characteristics and diagenetic stages of different lithologies within the Benxi Formation sandstone in the study area.

5.2.1.1 Eodiagenesis A

During the Late Carboniferous (310~240 million years ago), the sandstone reservoirs of the Benxi Formation in the study area were in the early diagenesis stage A. During this period, the basin underwent a phase of stable subsidence, with a burial depth generally less than 900 m and paleogeothermal temperatures below 65°C. The vitrinite reflectance (Ro) was below 0.35%, indicating the organic matter was in an immature stage (Hu et al., 2019). The presence of biotite and volcanic rock fragments in the sandstone underwent illitization and chloritization, resulting in an increase in reservoir alkalinity (Li et al., 2016). The decomposition of these minerals released Mg^{2+} and Fe^{2+} ions, facilitating the formation of thin films of chlorite along the grain boundaries.

During this stage, sedimentary materials underwent initial compaction, leading to a gradual increase in particle packing, while ductile lithic fragments deformed and filled the pore space. Primary intergranular pores were well-developed. At this stage, the reservoir had sufficient pore space, providing ample room for subsequent diagenetic processes.

5.2.1.2 Eodiagenesis B

During the Mid-Permian to Middle Jurassic period (240~210 million years ago), the sandstone of the Benxi Formation was in the early diagenesis stage B. During this period, the basin experienced

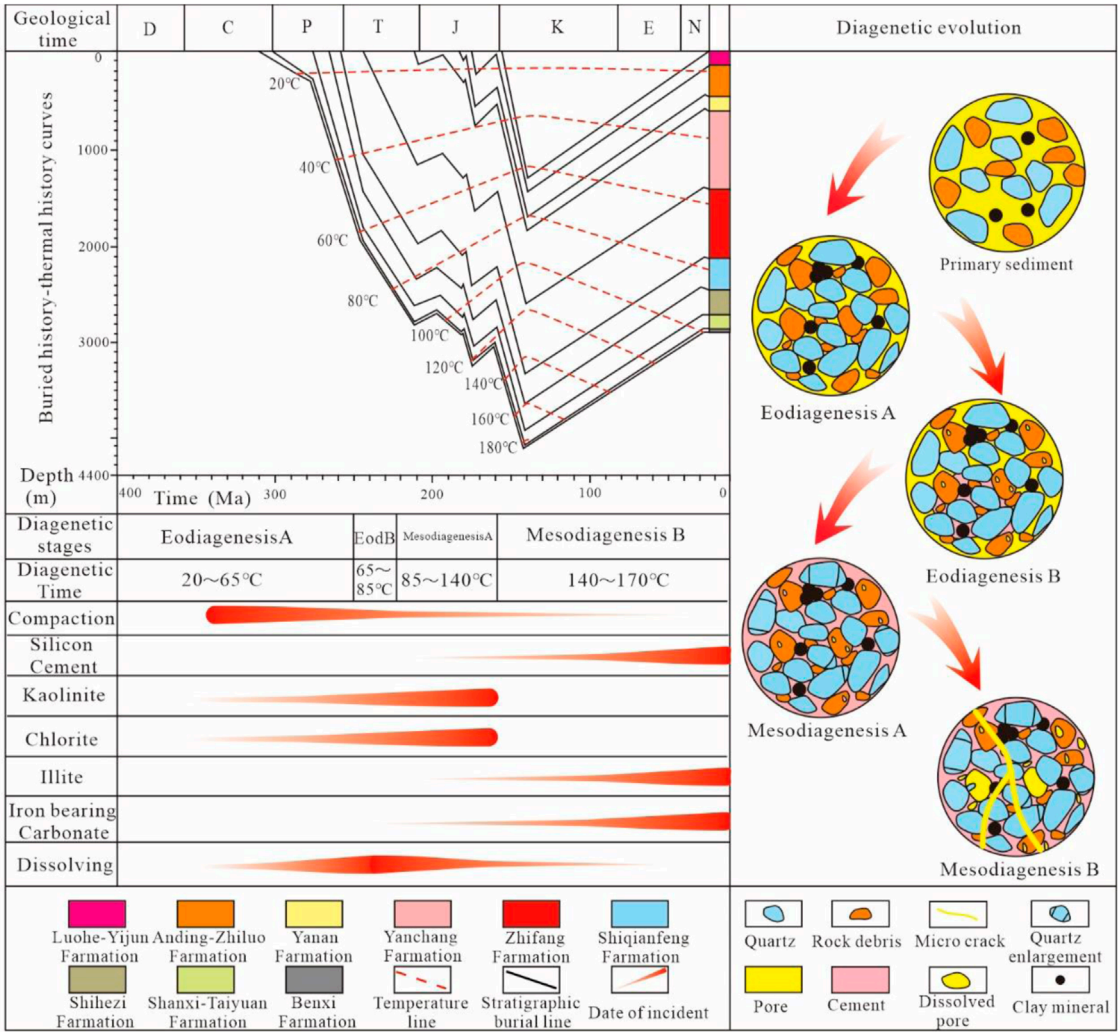

FIGURE 11
Diagram of rock~forming stages in the study area.

fluctuating subsidence, with burial depths ranging from 900 to 1800 m and paleogeothermal temperatures ranging from 65°C to 85°C. The vitrinite reflectance (Ro) values ranged from 0.35% to 0.5%, indicating the organic matter was in an immature to semi-mature stage (Hu et al., 2019). The primary diagenetic processes during this stage were compaction and the formation of siliceous and kaolinite cements. Due to the generation of organic acids, the pore fluids in the sandstone were acidic. Unstable components such as feldspar and lithic fragments underwent silicate mineral alteration, resulting in the precipitation of SiO_2 and the production of a small amount of HCO^{3-}. Under such acidic conditions, well-formed kaolinite cements precipitated and filled the intergranular pores (Li et al., 2016). Since fluid activity during this period was relatively weak, no corresponding hydrocarbon inclusions were captured in the sandstone.

During this period, sediment continued to settle, and compaction intensified, resulting in a continuous reduction of primary pores. Additionally, there was a short-term cementation process during this period, whereby some of the original intergranular pores were filled with cement, leading to a deterioration in reservoir quality.

5.2.1.3 Mesodiagenesis A

During the Late Jurassic to Early Cretaceous period (210~140 million years ago), the sandstone reservoir of the Benxi Formation entered the intermediate diagenesis phase A. At this time, the basin was still experiencing fluctuating subsidence, with burial depths ranging from 1800 to 4,100 m and paleogeothermal temperatures ranging from 85°C to 140°C. The vitrinite reflectance (Ro) values ranged from 0.5% to 1.3%, indicating the organic matter was in a low mature to mature stage (Hu et al., 2019). The main diagenetic processes during this period were kaolinite and siliceous cementation in the sandstone. Additionally, a first-stage oil and gas charging event occurred between 165 and 100 million years ago, corresponding to relatively low homogenization temperatures (120~130°C) of hydrocarbon inclusions. This event resulted in a large-scale distribution of oil and gas in primary fractures such as grain cracks, cleavage fractures, and various types of dissolution

pores and fractures in high-plastic rock debris sandstone, lithic quartz sandstone, and quartz sandstone.

This period was characterized by the most active organic-inorganic reactions between source rocks and reservoirs. The abundant organic and inorganic acid fluids formed during this time dissolved the unstable aluminosilicate minerals, clay minerals, and early cements in the Benxi sandstone, creating secondary porosity (Li et al., 2016). With increasing temperature and pressure conditions, the solubility of SiO_2 in the pore fluid increased, leading to the precipitation of siliceous cement within intergranular pores. Simultaneously, under acidic conditions, the dissolved kaolinite cement, derived from the dissolution of feldspar, filled the dissolution pores within the feldspar grains. As temperature and pressure continued to rise and organic acids were consumed, extensive dehydration of clay minerals occurred, resulting in the release of alkaline cations such as Na^+ and K^+ during the process of mineral dissolution and ion exchange. This increased the pH of the pore fluid, transitioning the diagenetic environment to a weak alkaline state. It also led to the transformation of illite/montmorillonite mixed layers and part of the kaolinite into illite. Additionally, a small amount of late-stage carbonate cementation occurred (Li et al., 2016).

During this period, the sediment was influenced by various diagenetic processes. The most significant influence was from compaction, which intensified with increasing depth. As a result, pore space was compressed, and the reservoir quality tended to become more tight. The period also experienced the first stage of acid leaching, where unstable components in the original sediment were dissolved by organic acids, creating a significant number of secondary pores. However, in the later stages of this period, the diagenetic environment transitioned to a weak alkaline condition, leading to the generation of a small amount of cement. This material filled the previously formed secondary pores, causing a deterioration in reservoir quality.

5.2.1.4 Mesodiagenesis B

During the Late Cretaceous (140~65 million years ago), the sandstone reservoir of the Benxi Formation entered the intermediate diagenesis phase B. At this time, the basin was undergoing tectonic uplift, with burial depths exceeding 3,100 m. The maximum burial depth was reached at the end of the Early Cretaceous, reaching 4,100 m. Paleogeothermal temperatures ranged from 140°C to 175°C, and vitrinite reflectance (Ro) values ranged from 1.3% to 2.0%, indicating the organic matter was in a highly mature stage (Hu et al., 2019). Due to the organic matter being highly mature, the kerogen had transformed into hydrocarbons, releasing a significant amount of organic acids and resulting in an acidic diagenetic environment. Late-stage carbonate cementation, formed during intermediate diagenesis phase A, was dissolved, leading to the occurrence of secondary dissolution during this period. Additionally, under high temperature, high pressure, and acidic conditions, illite transformed into kaolinite. A second-stage oil and gas charging event occurred between 90 and 70 million years ago, corresponding to relatively high homogenization temperatures (150~160°C) of hydrocarbon inclusions mentioned earlier.

During this period, there was structural uplift, and the effect of compaction weakened. As a result, some microfractures opened up, creating reservoir space. Additionally, the diagenetic environment transitioned to an acidic condition, causing the dissolution of later-formed carbonate cement, which resulted in the formation of numerous secondary dissolution pores. This led to an improvement in reservoir quality.

5.2.2 Mechanical compaction is the main cause of reservoir density

The Benxi Formation is in the middle stage of diagenesis, characterized by a prolonged period of mechanical compaction. The impact of compaction on reservoir quality can be attributed to the following factors:

(1) Compaction leads to the compression and densification of particles, resulting in a significant reduction in primary intergranular pores due to the particles' concave-convex contact.
(2) The presence of abundant ductile minerals, such as mica and shale fragments, within the lithic clasts can cause bending and deformation under pressure, filling the primary pore spaces and greatly reducing porosity and permeability.
(3) Intense compaction reduces the pore space, leading to complex pore-throat structures that hinder fluid entry, thereby inhibiting other diagenetic processes.

The outcome of diagenesis is the alteration of reservoir rock structure, composition, and storage capacity to some extent. The original porosity of reservoirs can be quantitatively estimated using empirical formulas based on porosity evolution models (Beard and Weyl, 1973). The calculation formula is as Eqs 1, 2:

$$\Phi = 20.91 + 22.9/S0 \quad (1)$$

$$S0 = P75/P25\% \quad (2)$$

The percentage of original porosity eliminated can be determined by Eqs 3, 4 (Huoseknecht, 1987):

$$\Phi ys = (\Phi - \Phi yy)/\Phi \quad (3)$$

$$\Phi jj = ((Vjjw)/\Phi) \times 100\% \quad (4)$$

Φ—Original pore volume; S0—Sorting coefficient; Φys—Compaction porosity loss rate; Φjj—Cementation porosity loss rate; Φyy—Core porosity; Vjjw—Cementation content.

By utilizing thin section identification data and petrophysical analysis data, parameters such as compacted porosity loss rate and cemented porosity loss rate can be calculated using appropriate formulas. These calculations help in assessing the extent to which different diagenetic processes affect reservoir properties (Figure 12A). In the studied area, compaction leads to a porosity loss of up to 80%, while cementation causes a porosity loss of approximately 10%. Therefore, mechanical compaction is the most significant diagenetic process affecting the quality of sandstone reservoirs in the study area and is also one of the primary reasons for their tightness.

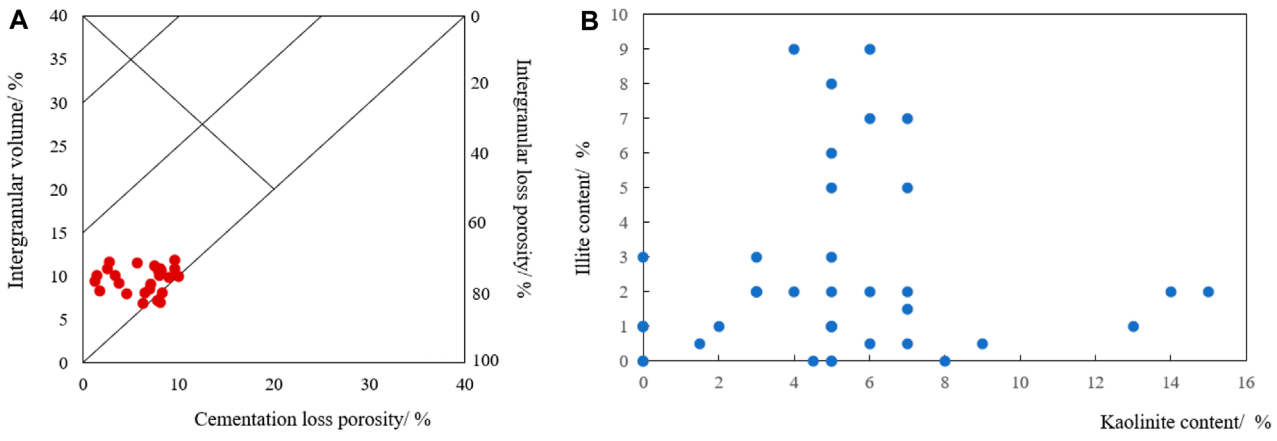

FIGURE 12
(A) Evaluation of the effect of cementation and compaction on porosity; **(B)** Correlation diagram between kaolinite and illite.

5.2.3 Silica cementation is the root cause of blocked pore throats

During the eodiagenesis to the mesodiagenesis stages of the Benxi Formation, sub-stances such as montmorillonite, kaolinite, and feldspar in the original sediments un-dergo mineral transformation and quartz grain dissolution due to increasing temper-ature and pressure (Hu et al., 2019). This process generates a certain amount of silica cement. The silica cements are relatively stable and, after their formation, they fill pores and block channels, resulting in a reduction in the size of the original wide and elongated pore structures and a change in pore structure type, thereby reducing the reservoir's storage capacity (Li et al., 2016). The silica cements primarily originate from the following two sources:

5.2.3.1 Mineral transformation process

The Benxi Formation belongs to terrestrial-marine tidal flat deposits, predominantly occurring in immersion areas such as the intertidal zone and subtidal zone (Peng et al., 2023). During the eodiagenesis, feldspar minerals experience increased burial depth which leads to gradual elevation in temperature and pressure. The initial hydrocarbon generation takes place at the top of the Benxi Formation, resulting in the production of abundant organic acids, thereby causing a shift towards an acidic diagenetic environment. Feldspar minerals combine with hydrogen ions to generate kaolinite, siliceous components, and sodium-potassium ions. Consequently, the content of silicates increases, culminating in the formation of siliceous cement after saturation. The chemical formula for the conversion of orthoclase feldspar into kaolinite is depicted as Eq. 5 (Li, Y et al., 2020):

$$2KAlSi_3O_8(F) + 2H^+ + H_2O \rightarrow Al_2Si_2O_5(OH)_4(K) + 4SiO_2 + 2K^+ \quad (5)$$

Significant dissolution of orthoclase feldspar only occurs when the temperature exceeds 90°C. At temperatures above 130°C, reaction between kaolinite and orthoclase feldspar takes place, resulting in the release of SiO_2, which aligns with the results obtained from fluid inclusion thermometry. The reaction can be described as Eq. 6 (Li et al., 2020):

$$Al_2Si_2O_5(OH)_4(K) + KAlSi_3O_8(F) \rightarrow KAlSi_3O_{10}(OH)_2(I) + 2SiO_2 + H_2O \quad (6)$$

In this reaction, kaolinite and orthoclase feldspar convert into illite and free SiO_2. The phenomenon of kaolinite illitization, accompanied by the presence of authigenic quartz grains, can be observed in Figure 13A, B. Moreover, the negative correlation between kaolinite and illite (Figure 12B), as well as the presence of data points exceeding 130°C in fluid inclusion thermometry results, provide evidence for this outcome.

During the mesodiagenesis, the second phase of hydrocarbon generation takes place in the upper coal layers of the Benxi Formation, resulting in the abundant release of organic acids. Illite is unstable and under high temperature and pressure conditions, it undergoes reverse transformation to become kaolinite. This phenomenon explains the higher content of kaolinite and lower content of feldspar minerals and illite in the Benxi Formation strata within the study area (Table 4).

5.2.3.2 Pressure dissolution of quartz particles

Pressure-solution provides a significant supply of silica for siliceous cementation, serving as a primary factor in secondary quartz overgrowth and interpenetration between particles (Figure 14A). In the study area, the burial depth of the Benxi Formation ranges from 2300 to 3400 m. With increasing temperature and pressure conditions, the pressure exerted on quartz grain contacts by overlying layers or laterally by tectonic stress exceeds the normal pore fluid pressure (Figure 14B). As a result, the solubility of quartz grain contacts increases, leading to lattice deformation and dissolution. The dissolved silica migrates with the pore water flow. When the pore water flows through low-pressure zones (Figure 14C), the reduced solubility of silica promotes crystal precipitation, resulting in the deposition of siliceous cement in intergranular pores.

10.3389/feart.2024.1377738

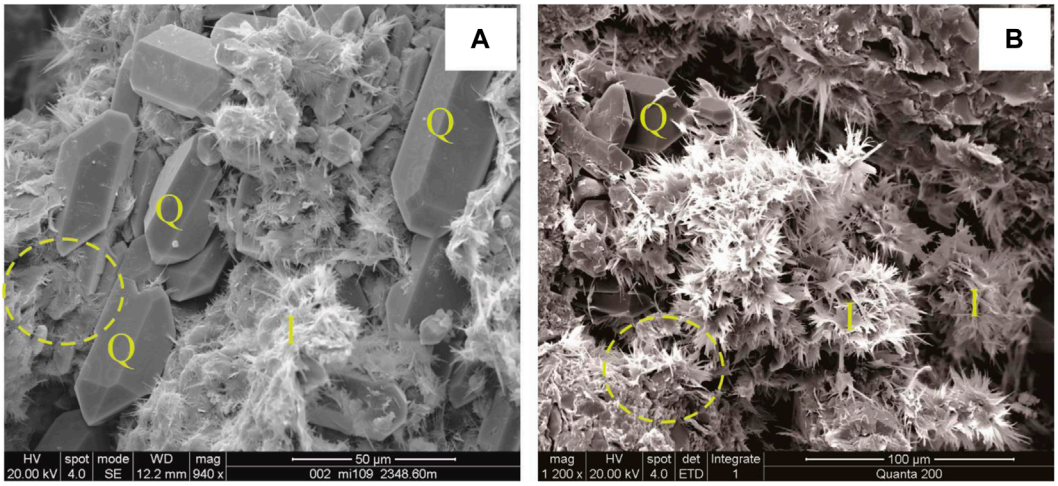

FIGURE 13
Kaolinite converts to illite and produces authigenic quartz. **(A)** Well M109, 2342m, SEM; **(B)** Well M128, 2042m, SEM. Q=Quartz, I=Illite.

TABLE 4 Clay mineral content table of different layers in the study area.

Stratum	Kaolinite	Illite	Chlorite	Reticulated clay	Total	Sample number
He 8	1.97	6.99	1.71	0.07	10.74	970
Shan 1	2.27	7.13	1.19	0.004	10.59	262
Shan 2	2.03	6.23	0.27	0.2	8.73	380
Taiyuan	1.03	9.77	0.36	0.04	11.2	142
Benxi	4.6	2.17	0.08	0	6.85	124

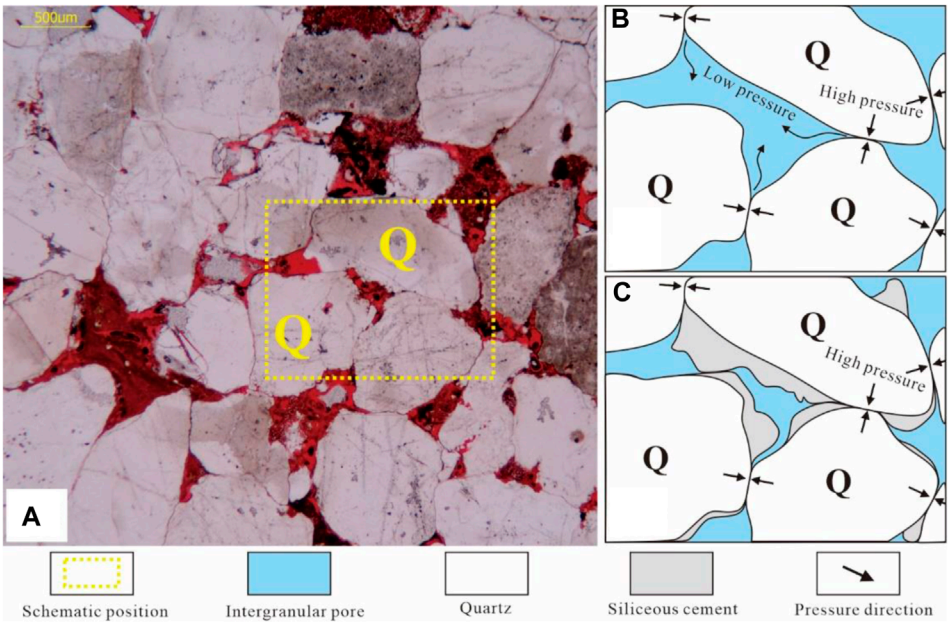

FIGURE 14
Micrographs showing compaction of quartz grains from the Benxi Formation. **(A)** Residual Intergranular Pores, Well M52, 2018m, (~); **(B)** Original contact state of quartz particles; **(C)** The current state of quartz particles. Q=Quartz.

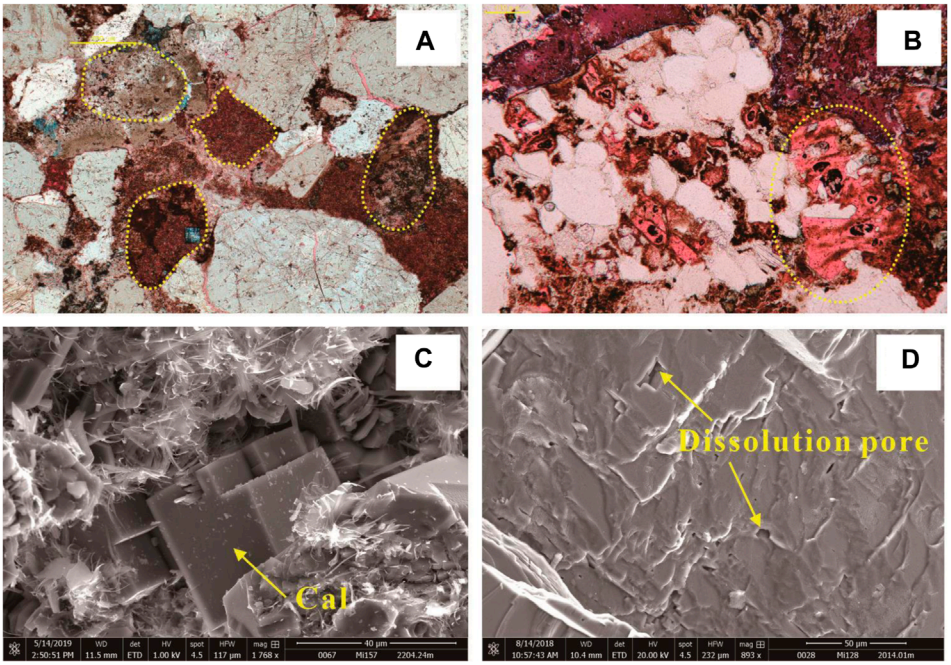

FIGURE 15
Micrographs showing compaction of quartz grains from the Benxi Formation. **(A)** Debris dissolution and cementation filling, Visible particle boundary morphology, Well M157, 2201 m, (~); **(B)** Late cementation is eroded, Well M110, 2101 m, (~); **(C)** The filling of calcite from pig iron can be seen in some pores, Well M157, 2204.24 m, SEM; **(D)** Residual Intergranular Pores, Well M128, 2014 m, SEM. Cal=Calcite.

5.2.4 Multi-phase dissolution is an important factor in reservoir porosity enhancement

For the majority of reservoirs, dissolution plays a crucial role in improving reservoir properties, and the secondary pores generated by dissolution are an important component of the rock storage space (Yuan et al., 2015). In the Benxi Formation, the thick coal rocks at the top act as the primary source of natural gas. During the process of coal generation and hydrocarbon expulsion, the organic acids produced infiltrate into the reservoir, creating a significant number of secondary pores. Fluid inclusion data from quartz overgrowths in the Benxi Formation indicate that the reservoir underwent two periods of gas charging, occurring at temperatures of 120~130°C and 150~160°C, respectively (Figure 8).

During the early stage of diagenesis, when the paleotemperature ranged from 120 to 130°C, the Benxi Formation experienced compaction to a lesser extent due to the high quartz content in the detrital materials, thereby preserving residual intergranular pores. Organic acids generated during this period entered the reservoir through these residual intergranular pores, causing dissolution of unstable feldspar and lithic fragments, resulting in the formation of secondary pores. Some of these secondary pores were later filled by subsequent mud or carbonate cementation (Figures 15A–C).

During the middle stage of diagenesis, when the paleotemperature reached 150~160°C, the Benxi Formation entered the B-stage of mesodiagenesis. The detrital materials underwent early mechanical compaction, followed by siliceous cementation in the intermediate stage, and late mud and iron carbonate cementation, leading to reservoir densification. During this period, the organic acids produced by coal rocks dissolved the later cements, creating a significant number of secondary pores, thus providing favorable storage space for natural gas accumulation (Figure 15D).

By using the dissolution porosity calculation formula Eqs 7, 8, it is estimated that the increased porosity due to dissolution in the Benxi Formation in the study area accounts for approximately 30%–40% of the total pore volume. Meanwhile, the primary intergranular porosity in the Benxi Formation accounts for only about 10%–20% of the total pore volume (Figure 16). This indicates that dissolution pores are the main reservoir space in the pore system of the Benxi Formation.

$$Vkx = Vrs + Vlj + Vqt \tag{7}$$

$$\Phi rs = ((Vrs)/Vkx) \times 100\% \tag{8}$$

Φ—Original pore volume; Φrs—Dissolution porosity; Vrs—Dissolution pore volume; Vlj—Intergranular pore volume; Vqt—Other pore volume; Vkx—total pore volume.

5.3 Comparative analysis

The reservoir quality of tight sandstone formations exhibits significant variations, as observed through a comparative analysis of different basins. It has been observed that the larger the grain size of tight sandstone reservoirs, the better their reservoir

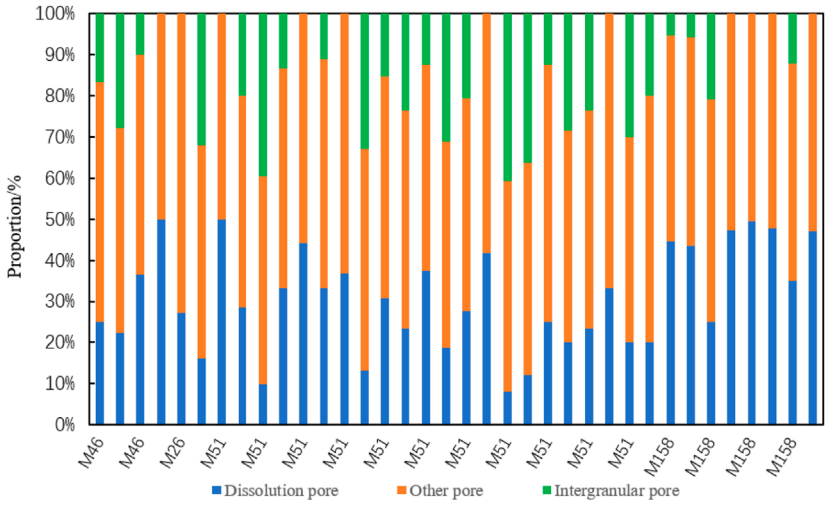

FIGURE 16
Percentage diagram of dissolved pore and intergranular pore.

TABLE 5 Reservoir quality differences of tight sandstone gas reservoirs in different basins.

Area	Reservoir type	Reservoir quality		Source
		Porosity (%)	Permeability ($\times10^{-3}$ μm^2)	
SichuanBasin, China	Fine and coarse grains	0.79~10.53	0.1	Huang et al. (2022)
Ordos Basin, China	Medium and coarse grains	0.23~13.77	1.35	This study
Tarim Basin, China	Fractured reservoir	2~8	0.1	Wang, J. P et al. (2023)
Yinggehai Basin, China	Medium grain	1.97~14.51	1.79	Zhao, X. B et al. (2022)
Songliao Basin, China	Argillaceous siltstone and sandstone	1.40~8.90	0.22	Xu, Z. J et al. (2020)

quality (Figures 9A, B). Additionally, if fractures form within the reservoir, the reservoir quality further improves. Fractures serve as favorable natural storage spaces for natural gas, with higher porosity and permeability compared to other types of reservoirs (Table 5).

5.4 Limitations

Although various methods and approaches were employed in this study, there are some limitations to be acknowledged. In the discussion of dissolution processes, the lack of experiments specifically focusing on organic acids was due to experimental constraints. Hence, only macroscopic descriptions of the dissolution effects from the two stages of acid leaching were provided, without quantitative characterization. Furthermore, the inclusion of experimental results from CT scans in the description of pore space types would have provided a clearer representation of the types and quantities of pore space within the reservoir, leading to more accurate research conclusions.

6 Conclusion

(1) Benxi Formation is mainly in the middle diagenetic B stage, which mainly undergoes compaction, cementation and dissolution. The two-stage acid discharge shown by fluid inclusions proves that there is two-stage dissolution, which is the fundamental reason for the increase of reservoir porosity.
(2) Based on the initial porosity recovery model and empirical formulas for compaction-induced porosity loss from the literature, thin section porosity analysis was used to determine that the original porosity of the Benxi Formation sandstone

is 39.8%, and compaction has led to a reduction in porosity of up to 80%. Cementation has caused a porosity decrease of 1.0%–5.4%, with an average of 4.1%. Compaction is the main reason for the widespread compactness in the study area's Benxi Formation.

(3) The rock type and source rock macroscopically influence pore evolution in the study area. Coarser-grained rocks with lower mud content have better original porosity and permeability. Compared to quartz sandstone, immature lithic sandstone and lithic quartz sandstone show stronger dissolution properties.

(4) Different diagenetic processes microscopically affect pore evolution in the study area. Stronger compaction leads to fewer pore spaces, limiting the modification of reservoirs by diagenetic fluids. Acidic cements formed by calcareous cement (such as illite) promote dissolution. Additionally, alkaline cements during late diagenesis also dissolve siliceous cements. Organic acids have a positive impact on dissolution, controlled by hydrocarbon expulsion. In conclusion, diagenesis has practical significance in predicting and exploring favorable areas for natural gas in the tight sandstones of the Benxi Formation.

Data availability statement

The original contributions presented in the study are included in the article/Supplementary material, further inquiries can be directed to the corresponding author.

Author contributions

GL: Conceptualization, Methodology, Writing–original draft, Writing–review and editing. CL: Investigation, Writing–original draft. Boming Zhang: Data curation, Writing–original draft. LZ: Writing–review and editing. ZL: Data curation, Writing–review and editing. QC: Writing–review and editing.

Funding

The author(s) declare that financial support was received for the research, authorship, and/or publication of this article. This work was supported by National Natural Science Foundation of China (No. 42172154).

Conflict of interest

Authors GL, CL, and BZ were employed by China National Petroleum Corp. Author LZ was employed by Luliang Oilfield Operation Area of Xinjiang Oilfield Branch Company.

The remaining authors declare that the research was conducted in the absence of any commercial or financial relationships that could be construed as a potential conflict of interest.

Publisher's note

References

Beard, D. C., and Weyl, P. K. (1973). Influence of texture on porosity and permeability of unconsolidated sand. *AAPG Bull.* 57 (2), 349–369. doi:10.1306/819A4272-16C5-11D7-8645000102C1865D

Colo n, C. F. J., Oelkers, E. H., and Schott, J. (2004). Experimental investigation of the effect of dissolution on sandstone permeability, porosity, and reactive surface area. *Geochem Cosmochim. Acta* 68 (4), 805–817. doi:10.1016/j.gca.2003.06.002

Crundwell, F. (2014). The mechanism of dissolution of minerals in acidic and alkaline solutions: Part II Application of a new theory to silicates, aluminosilicates and quartz. *Hydrometallurgy* 149 (11), 265–275. doi:10.1016/j.hydromet.2014.07.003

Dutton, S. P., and Loucks, R. G. (2010). Diagenetic controls on evolution of porosity and permeability in lower Tertiary Wilcox sandstones from shallow to ultradeep (200–6700 m) burial, Gulf of Mexico Basin, USA. *Mar. Petroleum Geol.* 27 (1), 69–81. doi:10.1016/j.marpetgeo.2009.08.008

Ehrenberg, S. (1990). Relationship between diagenesis and reservoir quality in sandstones of the Garn Formation, Haltenbanken, mid-Norwegian continental shelf. *AAPG Bull.* 74 (10), 1538–1558. doi:10.1306/0c9b2515-1710-11d7-8645000102c1865d

Ehrenberg, S., Nadeau, P., and Steen, Ø. (2009). Petroleum reservoir porosity versus depth: influence of geological age. *AAPG Bull.* 93 (10), 1281–1296. doi:10.1306/06120908163

Folk, W. (1957). A study in the significance of grain size parameters. *J. Sediment. Petrol.* 27, 3–27. doi:10.1306/74D70646-2B21-11D7-8648000102C1865D

Gao, Z. D. (2020). *Provenance analysis of Benxi Formation of upper carboniferous in Ordos Basin and distribution regularity of favorable sand bodies.* Chengdu: Chengdu University of Technology.

Hong, D. D., Cao, J., Wu, T., Dang, S. S., Hu, W. X., and Yao, S. P. (2020). Authigenic clay minerals and calcite dissolution influence reservoir quality in tight sandstones: insights from the central Junggar Basin, NW China. *Energy Geosci.* 1 (1-2), 8–19. doi:10.1016/j.engeos.2020.03.001

Hu, P., Yu, X. H., Chen, H. L., Zhao, C. F., Zhou, J. S., Han, X. Q., et al. (2019). Characteristics and a quantitative diagenetic porosity evolution mode of barrier bar sandstone reservoirs: a case study of the Benxi Formation, Yanchang exploration block, Ordos Basin. *Acta Sedimentol. Sin.* 37 (02), 390–402. doi:10.14027/j.issn.1000-0550.2018.121

Huang, Y., Wang, A., Xiao, K., Lin, T., and Jin, W. (2022). Types and genesis of sweet spots in the tight sandstone gas reservoirs: insights from the Xujiahe Formation, northern Sichuan Basin, China. *Energy Geosci.* 3 (3), 270–281. doi:10.1016/j.engeos.2022.03.007

Huoseknecht, D. W. (1987). Assessing the relative importance of compaction processes and cementation to reduction of porosity in sandstone. *AAPG Bull.* 71 (3), 633–642. doi:10.1306/9488787F-1704-11D7-8645000102C1865D

Jia, L. B., Zhong, D. K., Ji, Y. L., Zhou, Y., Liu, J. L., Mi, L. J., et al. (2019a). Architecture of tectonic sequences, depositional systems, and tectonic controls of the sedimentary fills of the riftrelated Wenchang Formation in the Lufeng Depression, Pearl River Mouth Basin, China. *Geol. J.* 54 (4), 1950–1975. doi:10.1002/gj.3272

Jia, L. B., Zhong, D. K., Sun, H. T., Zhang, C., Mo, W., Qiu, C., et al. (2019b). Sediment provenance analysis and tectonic implication of the Benxi Formation, Ordos Basin. *Acta Sedimentol. Sin.* 37 (5), 1087–1103. doi:10.14027/j.issn.1000-0550.2019.014

Li, J., Zhang, C. L., Jiang, F. J., Pei, Y., Wang, J. Y., Wang, X. R., et al. (2021). Main factors controlling the enrichment of upper caiboniferous Benxi Formation tight gas in the Ordos Basin. *Nat. Gas. Ind.* 41 (04), 30–40. doi:10.3787/j.issn.1000-0976.2021.04.004

Li, M., Hou, Y. D., Luo, J. L., Chen, J. P., Luo, X. R., and Jia, Y. N. (2016). Quantitative analysis of burial-diagenesis-hydrocarbon charging evolution process and pore evolution of tight sandstone reservoirs - a case study of natural gas reservoirs in the Upper Paleozoic He 8 Member in the eastern Ordos Basin. *Oil Gas Geol.* 37 (06), 882–892. doi:10.11743/ogg20160610

Li, Y., Xu, W. K., Wu, P., and Meng, S. Z. (2020). Dissolution versus cementation and its role in determining tight sandstone quality: a case study from the Upper Paleozoic in northeastern Ordos Basin, China. *J. Nat. Gas Sci. Eng.* 78, 103324. doi:10.1016/j.jngse.2020.103324

Lin, J., Li, Y., and He, J. (2013). An analysis of the source and the sedimentary system of the carboniferous Benxi Formation in yanchang area of Ordos Basin. *Geol. China* 40 (5), 1542–1551.

Morad, S., Al-Ramadan, K., Ketzer, J. M., and De Ros, L. (2010). The impact of diagenesis on the heterogeneity of sandstone reservoirs: a review of the role of depositional facies and sequence stratigraphy. *AAPG Bull.* 94, 1267–1309. doi:10.1306/04211009178

Panagiotopoulou, C., Kontori, E., Perraki, T., and Kakali, G. (2007). Dissolution of aluminosilicate minerals and by-products in alkaline media. *Mat. Sci.* 42 (9), 2967–2973. doi:10.1007/s10853-006-0531-8

Paxton, S., Szabo, J., Ajdukiewicz, J., and Klimentidis, R. (2002). Construction of an intergranular volume compaction curve for evaluating and predicting compaction and porosity loss in rigid-grain sandstone reservoirs. *AAPG Bull.* 86 (0), 2047–2067. doi:10.1306/61eeddfa-173e-11d7-8645000102c1865d

Peng, Z. X., Yu, X. H., Li, S. L., Qi, R., Fu, C., and Jiang, L. Y. (2023). Barrier migration patterns and controlling factors of Benxi Formation in southeastern Ordos Basin. *J. Palaeogeogr.* 25 (06), 1330–1346. doi:10.7605/gdlxb.2023.06.092

Pokrovsky, O. S., Golubev, S. V., Schott, J., and Castillo, A. (2009). Calcite, dolomite and magnesite dissolution kinetics in aqueous solutions at acid to circumneutral pH, 25 to 150 °C and 1 to 55 atm pCO2: new constraints on CO2 sequestration in sedimentary basins. *Chem. Geol.* 265 (1-2), 20–32. doi:10.1016/j.chemgeo.2009.01.013

Scherer, M. (1987). Parameters influencing porosity in sandstones: a model for sandstone porosity prediction. *AAPG Bull.* 71 (5), 485–491. doi:10.1306/94886ed9-1704-11d7-8645000102c1865d

Taylor, T. R., Giles, M. R., Hathon, L. A., Diggs, T. N., Braunsdorf, N. R., Birbiglia, G. V., et al. (2010). Sandstone diagenesis and reservoir quality prediction: models, myths, and reality. *AAPG Bull.* 94 (8), 1093–1132. doi:10.1306/04211009123

Wang, F., Liu, X. C., Deng, X. Q., Li, Y. H., Tian, J. C., Li, S. Y., et al. (2017). Geochemical characteristics and environmental implications of trace elements of Zhifang Formation in Ordos Basin. *Acta Sedimentol. Sin.* 35 (6), 1265–1273. doi:10.14027/j.cnki.cjxb.2017.06.017

Wang, J., Zhang, C. L., and Li, J. (2021a). Tight sandstone gas reservoirs in the Sulige gas field: development understandings and stable production proposals. *Nat. Gas. Ind.* 41 (02), 100–110. doi:10.3787/j.issn.1000-0976.2021.02.012

Wang, J. P., Wang, H. Y., Zhang, R. H., Li, D., Wang, K., and Zhang, Z. Y. (2023). Improvement of reservoir quality of ultra-deep tight sandstones by tectonism and fluid: a case study of Keshen gas field in Tarim Basin, western China. *Petroleum* 9 (1), 124–134. doi:10.1016/j.petlm.2023.01.002

Wang, J. Y., Jiang, F. J., Zhang, C. L., Song, Z. Z., and Mo, W. L. (2021b). Study on the pore structure and fractal dimension of tight sandstone in coal measures. *Energy Fuel* 35, 3887–3898. doi:10.1021/acs.energyfuels.0c03991

Wang, X., Hou, J., Li, S., Dou, L., Song, S., Kang, Q., et al. (2020a). Insight into the nanoscale pore structure of organic-rich shales in the Bakken Formation, USA. *J. Petroleum Sci. Eng.* 176, 107182–107320. doi:10.1016/j.petrol.2020.107182

Wang, X., Liu, Y., Hou, J., Li, S., Kang, Q., Sun, S., et al. (2020b). The relationship between synsedimentary fault activity and reservoir quality — a case study of the Ek1 formation in the Wang Guantun area, China. *China. Interpret.* 8, sm15–sm24. doi:10.1190/INT-2019-0131.1

Wang, X., Yu, S., Li, S., and Zhang, N. (2022). Two parameter optimization methods of multi-point geostatistics. *J. Petroleum Sci. Eng.* 208, 109724. doi:10.1016/j.petrol.2021.109724

Wang, X., Zhang, F., Li, S., Dou, L., Liu, Y., Ren, X., et al. (2021c). The architectural surfaces characteristics of sandy braided river reservoirs, case study in gudong oil field, China. *Geofluids* 2021, 1–12. doi:10.1155/2021/8821711

Xu, Z. J., Jiang, S., Liu, L. F., Wu, K. J., Li, R., Liu, Z. Y., et al. (2020). Natural gas accumulation processes of tight sandstone reservoirs in deep formations of Songliao Basin, NE China. *J. Nat. Gas Sci. Eng.* 83, 103610. doi:10.1016/j.jngse.2020.103610

Yuan, G. H., Cao, Y. C., Gluyas, J., Li, X. Y., Xi, K. L., Wang, Y. Z., et al. (2015). Feldspar dissolution, authigenic clays, and quartz cements in open and closed sandstone geochemical systems during diagenesis: typical examples from two sags in Bohai Bay Basin, East China. *AAPG Bull.* 99 (11), 2121–2154. doi:10.1306/07101514004

Zhang, C. L., Sun, W., Gao, H., Xi, T. D., He, Q. Y., Shi, J. C., et al. (2014). Quantitative calculation of sandstone porosity evolution based on thin section data: a case study from Chang 8 reservoir of Huanjiang Area, Ordos Basin. *Acta Sedimentol. Sin.* 32 (02), 365–375. doi:10.14027/j.cnki.cjxb.2014.02.021

Zhao, X. B., Yao, G. Q., Chen, X. J., Zhang, R. X., Lan, Z. J., and Wang, G. C. (2022). Diagenetic facies classification and characterization of a high-temperature and high-pressure tight gas sandstone reservoir: a case study in the Ledong area, Yinggehai Basin. *Mar. Petroleum Geol.* 140, 105665. doi:10.1016/j.marpetgeo.2022.105665

Zhong, D. K., Zhu, X. M., Zhou, X. Y., and Wang, Z. M. (2007). An approach to categories and mechanisms of SiO2 dissolution in sandstone reservoirs in the Tarim Basin. *Chin. J. Geol. Geol. Sinica* 42 (02), 403–414.